

ODI-BENCH: CAN MLLMS UNDERSTAND IMMERSIVE OMNIDIRECTIONAL ENVIRONMENTS?

Liu Yang^{1,*}, Huiyu Duan^{1,*}, Ran Tao², Juntao Cheng¹, Sijing Wu¹, Yunhao Li¹, Jing Liu³, Xionghuo Min¹, Guangtao Zhai¹

¹Shanghai Jiao Tong University

²Xinjiang University

³Tianjin University



Figure 1: (a) We introduce **ODI-Bench**, a comprehensive benchmark for omnidirectional image understanding, covering 10 diverse tasks. (b) 20 leading MLLMs are benchmarked with both close-ended and open-ended evaluation. (c) To further improve model performance, we propose **Omni-CoT**, a chain-of-thought framework that enhances MLLMs’ comprehension on omnidirectional images via step-by-step reasoning.

ABSTRACT

Omnidirectional images (ODIs) provide full $360^\circ \times 180^\circ$ view which are widely adopted in VR, AR and embodied intelligence applications. While multi-modal large language models (MLLMs) have demonstrated remarkable performance on conventional 2D image and video understanding benchmarks, their ability to comprehend the immersive environments captured by ODIs remains largely unexplored. To address this gap, we first present **ODI-Bench**, a novel comprehensive benchmark specifically designed for omnidirectional image understanding. ODI-Bench contains 2,000 high-quality omnidirectional images and over 4,000 manually annotated question-answering (QA) pairs across 10 fine-grained tasks, covering both general-level and spatial-level ODI understanding. Extensive experiments are conducted to benchmark 20 representative MLLMs, including proprietary and open-source models, under both *close-ended* and *open-ended* settings. Experimental results reveal that current MLLMs still struggle to capture the immersive context provided by ODIs. To this end, we further introduce **Omni-CoT**, a training-free method which significantly enhances MLLMs’ comprehension ability in the omnidirectional environment through chain-of-thought reason-

*Equal contribution.

†Corresponding authors.

Table 1: Comparison between widely adopted general benchmarks, omnidirectional benchmarks, and our ODI-Bench. The first row group presents commonly used image benchmarks, the middle row group includes two spatial benchmarks, and the last row group lists ODI benchmarks.

Benchmark	#Images	#QA Pairs	#Question Type	Visual Modality	Max Reso.	Real Scenes	Evaluation		Dimension		QA Source
							Open	Close	General	Spatial	
MMBench (Liu et al., 2024b)	3,217	3,217	20	2D image	<1K	✓	✗	✓	✓	✗	Manual
MM-Vet (Yu et al., 2023)	200	218	16	2D image	<6K	✓	✓	✗	✓	✓	Manual&Existed
ViewSpatial-Bench (Li et al., 2025)	1,000	5,700	5	3D Scene	<1K	✓	✓	✗	✗	✓	Auto
VSI-Bench (Yang et al., 2025a)	29	5,000	8	NFOV Video	<1K	✓	✓	✗	✗	✓	Auto
SSRBench (Liu et al., 2025)	789	789	6	2D Image	-	✓	✓	✓	✓	✓	Auto
VQA 360° (Chou et al., 2020)	1,490	17,000	6	Indoor ODI	1K	✗	✗	✓	✓	✓	Auto
OSR-Bench (Dongfang et al., 2025)	4,100	153,000	3	Indoor ODI	1K	✗	✓	✗	✗	✓	Auto
Dense360-Bench (Zhou et al., 2025)	1,279	6,000	2	Indoor&Outdoor ODI	-	✓	✓	✗	✓	✗	Auto
ODI-Bench (Ours)	2,000	4,254	10	Indoor&Outdoor ODI	12K	✓	✓	✓	✓	✓	Manual&Auto

ing across both textual information and visual cues. Both the benchmark and the code will be released at <https://github.com/IntMeGroup/ODI-Bench>.

1 INTRODUCTION

360° omnidirectional images (ODIs) have gained increasing attention nowadays. Unlike conventional 2D images with limited field of views (FoVs), ODIs provide a full $180^\circ \times 360^\circ$ FoV with rich scene information, enabling fully immersive viewing. Thus, ODIs are widely used in virtual reality (VR), augmented reality (AR), spatial navigation, and hold great potential for embodied intelligence (Yang et al., 2025b; Zheng et al., 2025). Although recent advances in multi-modal large language models (MLLMs) have led to significant progress in conventional image understanding across various benchmarks (Liu et al., 2024b; Yu et al., 2023), their ability to comprehend ODIs has not been comprehensively evaluated, with existing benchmarks remaining insufficient. Compared to conventional images, ODIs capture substantially richer visual information from omnidirectional scenes and require higher-level spatial reasoning in immersive environments beyond a single front-view perspective. These unique characteristics make ODI understanding a distinct and difficult research challenge, highlighting the necessity to systematically evaluate MLLMs on this task.

Though a limited number of ODI understanding benchmarks have been proposed as shown in Table 1, they generally suffer from one or more of the following issues: (1) **Low resolution**: since many applications (such as VR, autonomous driving) requires high-resolution ODIs to provide immersive viewing experience or 360° details, benchmarks with low resolution are impractical for real-world application (Chou et al., 2020; Dongfang et al., 2025); (2) **Limited scene diversity**: some benchmarks are developed with the assistance of 3D-annotated indoor datasets (Chou et al., 2020; Dongfang et al., 2025), focusing only on indoor environments, or even unrealistic synthetic indoor scenes with blurry top-bottom views; (3) **Constrained question domains**: Existing benchmarks are automatically annotated, either leveraging existing 3D datasets or curated pipelines for question generation, thus tend to exhibit strong textual biases and provide relatively narrow or simplistic question types (Zhou et al., 2025); (4) **Viewpoint limitation**: for spatial understanding, existing ODI benchmarks are primarily designed from an egocentric perspective, neglecting allocentric viewpoints and the simulation of user interactions. As a result, they fall short in evaluating the embodied aspects of spatial understanding, which are critical for advancing embodied intelligence and interactive multimodal systems.

To address these gaps, we introduce **ODI-Bench**, a novel ODI-oriented benchmark designed to comprehensively evaluate both the general-level and spatial-level understanding capabilities of MLLMs. The question–answer pairs are derived from two complementary sources: (1) a rigorously designed automated pipeline that generates reliable instance-level QA pairs, which are further checked and refined by human experts, and (2) high-quality human annotations produced by three domain experts, whose works are carefully cross-checked to ensure reliability. The final benchmark contains 2,000 high quality real-life omnidirectional images, covering diverse indoor and outdoor scenes. 10 representative tasks are proposed to facilitate fine-grained and multi-perspective evaluation of the performance of MLLMs under ODI settings, partially illustrated in Figure 1.

Unlike previous benchmarks that restrict the evaluation of each task to either a close-ended (multiple-choice or true/false) or an open-ended QA setting, **ODI-Bench** evaluates every task under *both* settings. This dual-format design enables a comprehensive and comparative assessment, capturing both the recognition accuracy under constrained choice conditions and the model’s generative reasoning ability in unconstrained scenarios. Experimental results demonstrate that MLLMs still struggle to comprehend the immersive environment presented by ODIs. To this end, we further propose a training-free chain-of-thought framework, termed **Omni-CoT**, to improve MLLMs’ understanding capabilities on ODIs through step-by-step reasoning with viewpoint-guided scene

interpretation and visual cue based refinement. This approach significantly enhances MLLMs’ comprehension on ODIs across both general and spatial-level tasks. Our contributions are summarized as follows:

- We introduce **ODI-Bench**, a comprehensive benchmark for evaluating MLLMs on omnidirectional image understanding, which consists of 2,000 high-quality omnidirectional images and over 4,000 QA pairs across 10 fine-grained tasks, covering both general and spatial-level ODI understanding.
- We conduct an in-depth study to evaluate the ODI comprehension ability of 20 leading MLLMs on our ODI-Bench, using both close-ended and open-ended settings to make comprehensive and comparative analysis. Experimental results reveal the challenges of MLLMs in understanding immersive ODI scenes.
- We propose **Omni-CoT**, a training free strategy to enhance MLLMs’ comprehension capabilities on omnidirectional scenes through chain-of-thought reasoning. Experimental results demonstrate the effectiveness of the proposed framework on both proprietary and open-sourced models.

2 RELATED WORKS

2.1 GENERAL UNDERSTANDING BENCHMARKS

With the advancement of MLLMs, there is an increasing need for comprehensive and systematic evaluation of their visual understanding capabilities. A number of benchmarks have been developed to assess the general-level comprehension ability of MLLMs (Liu et al., 2024b; Yu et al., 2023; Duan et al., 2025). However, as the performance of MLLMs has significantly improved, such general benchmarks are no longer sufficient for thorough ability assessment. More recently, new benchmarks are proposed to evaluate the spatial understanding ability of MLLMs (Yang et al., 2025a; Liu et al., 2025), presenting new challenges for MLLMs on spatial understanding tasks. However, while most of these benchmarks focus on 2D images or N FoV videos, the benchmarks specifically designed for omnidirectional images are still scarce. Given their unique format and application scenarios, the ability to understand ODIs holds great potential for advancing not only MLLMs but also vision-language-action (VLA) models.

2.2 OMNIDIRECTIONAL IMAGE UNDERSTANDING BENCHMARKS

A limited number of ODI understanding benchmarks are proposed to evaluate MLLMs’ understanding of this unique type of images. Dense360-Bench (Zhou et al., 2025) introduces a QA curation pipeline and further constructs a benchmark for general-level grounding and captioning tasks on ODIs, but such tasks remain superficial and fall short in adequately evaluating spatial understanding abilities. VQA 360° (Chou et al., 2020) constructs a benchmark for simple ODI understanding tasks, but the image resolution is too low (1024×512), constraining its applicability in real-world scenarios. OSR-Bench (Dongfang et al., 2025) develops a pipeline for generating ODI spatial comprehension QA pairs from 3D datasets, yet it focuses solely on synthetic low-resolution indoor scenes, limiting its applicability. In contrast, our ODI-Bench is the first to comprehensively benchmark both the general-level and spatial understanding capabilities of MLLMs on ODIs, with carefully manually curated QA-pairs assisted by an automatic annotation pipeline, encompassing both high-quality indoor and outdoor scenes.

3 ODI-BENCH

3.1 OVERVIEW OF ODI-BENCH

In this section, we introduce **ODI-Bench**, a benchmark for comprehensive evaluation of MLLMs on omnidirectional image understanding. ODI-Bench consists of 2,000 real-world omnidirectional images covering diverse indoor and outdoor scenes, along with 4,254 question-answering pairs across 10 fine-grained tasks, offering both general-level and spatial-level ODI understanding evaluation.

3.2 IMAGE COLLECTION

The images in our benchmark are primarily web-crawled from Flickr and carefully selected to ensure both quality and diversity. The distribution of images is presented in Figure 2 (a) and (b). Compared with existing omnidirectional image understanding benchmarks (Dongfang et al., 2025; Chou

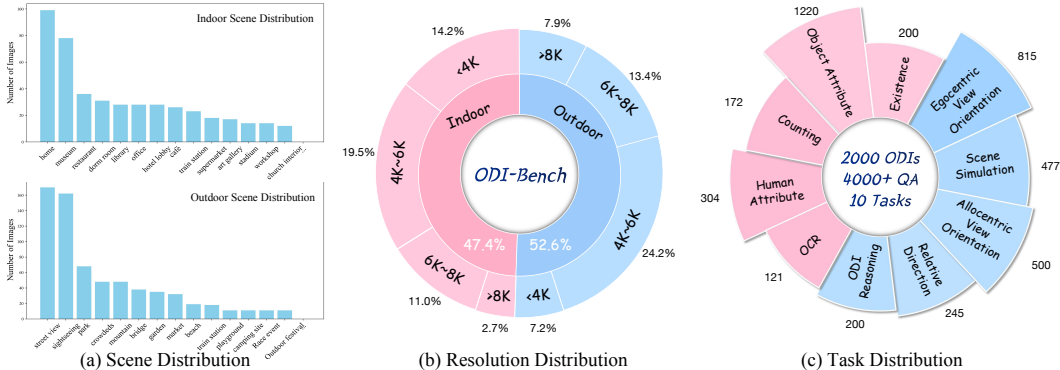


Figure 2: Data distribution in ODI-Bench.

et al., 2020) which are largely restricted to indoor environments and predominantly depict house-like scenes rendered from 3D datasets, our benchmark covers diverse indoor and outdoor scenes, ranging from human activity to natural landscapes, hereby enabling a comprehensive evaluation across diverse scenarios. In addition, some existing benchmarks suffer from low image quality. For instance, VQA 360° (Chou et al., 2020) consists of ODIs with blurry top and bottom views and the image resolutions are limited to 1K, which restricts their practical value in real-world applications. In contrast, as presented in Figure 2 (b), our benchmark is high quality, with sufficient resolution to ensure both practical applicability and reliable benchmarking.

3.3 FINE-GRAINED TASK DEFINITION

Unlike previous works that evaluate MLLMs’ comprehension abilities on ODIs either at the general level (Zhou et al., 2025) or the spatial level (Dongfang et al., 2025), or through a simple combination of the two (Chou et al., 2020), we carefully design 10 fine-grained tasks tailored for comprehensive ODI understanding, covering both general-level and spatial-level aspects, as shown in Figure 2.

General-level ODI understanding. Inspired by conventional 2D image understanding tasks, we propose five main general-level tasks to evaluate MLLMs’ comprehension on common ODI scenarios. These tasks typically impose relatively low spatial reasoning requirements, while the main challenges arise from the massive amount of visual information and distorted projections inherent in ODIs. Among them, we define instance-level tasks, i.e., *object-attribute* and *human-attribute*, to assess the models’ ability to accurately localize instances and extract visual information across wide fields of view. In addition, we introduce *counting* and *existence* tasks to measure the models’ global perception capabilities on omnidirectional images. Finally, we define a omnidirectional *OCR* task to evaluate the models’ capability to extract textual information under distorted perspectives and high-resolution conditions, including cross-view scenarios.

Spatial-level ODI understanding. Omnidirectional images project immersive 3D scenes onto a 2D plane, leading to substantial differences in spatial perception compared to conventional 2D images. In 2D images, the viewer is constrained to a single front-facing perspective, while ODIs provide a full 360° field of view encompassing front, back, left, right, top, and bottom perspectives. To evaluate the capability of MLLMs in handling such unique spatial characteristics, we design dedicated spatial-level ODI understanding tasks. These include *egocentric view orientation* and *relative direction* tasks, which adopt the viewer’s own perspective, as well as *allocentric view orientation* and *scene simulation* tasks, which involve perspective-taking from another agent or a virtual viewpoint. Furthermore, due to the equirectangular projection (ERP) format of ODIs, spatial relationships and motion trajectories often become distorted and confusing. To address this, we introduce an ODI-reasoning task, specifically designed to assess MLLMs’ ability to understand and interpret ERP-related spatial properties in ODIs, as illustrated in Figure 1.

3.4 QUESTION-ANSWERING ANNOTATION

Instead of conventional phrasing in 2D images benchmarks (e.g., “What is [A] on the right side of the image doing?”), we adopt an *immersive question design* tailored to the characteristics of omnidirectional images, i.e., “What is [A] on my right doing?”. This first-person phrasing not only aligns with the natural immersive viewing experience of ODIs but also serves to evaluate the ability

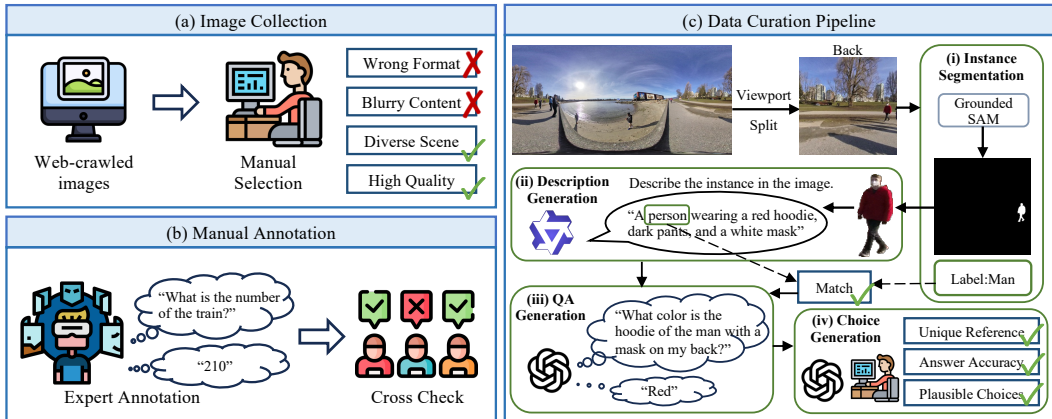


Figure 3: Construction procedures of ODI-Bench. (a) The benchmark images are carefully selected to ensure quality and diversity. (b) The majority tasks are manually annotated by human experts. (c) Object Attribute and Human Attribute QA pairs are generated through a dedicated annotation pipeline with human verification to guarantee quality.

of MLLMs to understand and utilize ODIs in interactive environments. For the QA construction process, we adopt both automatic pipelines and manual annotation process for different tasks.

For instance-level QA generation, *i.e.*, object attribute and human attribute, an automatic pipeline is adopted as presented in Figure 3. The ERP-formatted image is first cubemap-projected into 6 non-overlapping viewpoints for lower distortion. After that, GroundedSAM (Ren et al., 2024) is adopted to segment instances in each view, producing both segmentation masks and instance labels. To ensure precise instance segmentation, instances spanning multiple views are filtered out. The remaining instances are cropped based on the segmentation masks and fed into Qwen2.5-VL-72B (Bai et al., 2025b) for detailed caption. To ensure reliable instance selection, only those instances whose predicted categories by GroundedSAM are consistent with the descriptions from Qwen-VL-72B are retained. These captions are further utilized by GPT-4o to generate QA pairs. All the generated QAs are manually refined to ensure (i) unique reference, so that each question clearly targets a single instance; (ii) answer accuracy, guaranteeing the correctness of the provided answers.

For more complex tasks including counting, view-orientation and relative direction, *etc.*, automatic generation is not trust-worthy enough, thus manual annotation is employed for precision. The annotation process took one month in VR environments with three expert participants, whose annotations were cross-checked to guarantee accuracy. To construct close-ended evaluation, GPT-4o is adopted to generate 3 distractor options based on the QA pairs and the corresponding omnidirectional images. Each multiple-choice question is accompanied by three distractors, which are further assessed by human annotators to ensure their plausibility and to avoid semantic overlap with the correct answer. To mitigate model bias, the options are randomly shuffled, thereby ensuring a balanced distribution of correct answers across choices A to D.

4 EXPERIMENT

4.1 EVALUATION SETUP

We conduct comprehensive experiments on 20 leading MLLMs with different architectures and parameter scales on our ODI-Bench. The models can be categorized into two groups: (1) proprietary models, including GPT-4o (Hurst et al., 2024), o3 (OpenAI, 2025), Gemini (Comanici et al., 2025), *etc.* (2) open-sourced models, including InternVL series (Zhu et al., 2025), Qwen-VL series (Bai et al., 2025b), LLaVA-NeXT (Li et al., 2024b), LLaVA-OneVision (Li et al., 2024a), *etc.* All models are evaluated using the same prompt template provided in the Appendix.

We believe that model performance may vary under different evaluation settings, *i.e.*, close-ended and open-ended conditions. Unlike prior benchmarks, we benchmark all models across all tasks using both close-ended formats (multiple-choice or yes/no) and open-ended formats, providing a comprehensive and comparative assessment of their capabilities. For close-ended benchmark, model performances are measured by their accuracy on multi-choice or yes/no questions. For open-ended benchmark, we adopt the *LLM-based evaluator* (Yu et al., 2023), as detailed in the Appendix E.3. Finally, we report the average score for each task.

Table 2: Benchmark results for MLLMs under the close-ended evaluation setting. The tasks are defined as follows: OA (Object Attribute), HA (Human Attribute), Exist. (Existence), Count. (Counting), EVO (Egocentric View Orientation), AVO (Allocentric View Orientation), SS (Scene Simulation), RD (Relative Direction), OR (ODI Reasoning). For each task, the **best-performance** is indicated in bold and the second-best are underlined.

	Overall	General					Spatial				
		OA	HA	Exist.	Count.	OCR	EVO	AVO	SS	RD	OR
<i>Proprietary MLLMs</i>											
GPT-4o (Hurst et al., 2024)	55.79	74.43	<u>67.76</u>	65.50	49.42	74.38	43.24	32.49	39.60	57.55	53.50
Qwen-VL-Plus (Bai et al., 2025b)	53.85	<u>74.51</u>	68.75	43.00	<u>52.33</u>	67.77	46.13	29.98	34.80	50.61	49.00
Gemini-2.0-flash (Comanici et al., 2025)	<u>57.12</u>	73.03	<u>69.41</u>	<u>66.50</u>	52.33	80.16	<u>48.10</u>	<u>32.91</u>	<u>40.20</u>	<u>61.13</u>	<u>54.00</u>
o3 (OpenAI, 2025)	62.62	75.82	74.01	75.00	57.56	<u>77.69</u>	56.20	39.62	46.60	70.20	59.50
<i>Open-sourced MLLMs</i>											
LLaVA-v1.5-7B (Liu et al., 2024a)	45.04	64.02	51.44	58.00	34.30	42.15	43.86	28.93	19.60	24.08	50.00
LLaVA-ov-0.5B (Li et al., 2024a)	44.25	61.21	61.26	42.00	44.77	27.27	30.61	29.77	35.40	50.20	32.00
idefics3-8B (Laurençon et al., 2024)	49.89	68.45	65.32	62.50	50.00	57.85	36.71	28.79	30.20	49.39	49.50
XComposer2 (Dong et al., 2024)	51.84	75.57	<u>76.32</u>	44.00	54.07	25.62	46.56	32.29	27.20	31.84	46.00
Deepseek-VL-1.3B (Lu et al., 2024)	42.02	55.66	50.00	52.50	39.53	29.75	39.02	28.18	28.00	32.27	49.00
LLaVA-Next-7B (Li et al., 2024b)	45.91	64.84	54.93	60.50	39.77	45.45	40.42	27.04	21.20	32.24	53.50
LLaVA-Next-34B (Li et al., 2024b)	52.24	70.57	62.17	54.50	45.93	45.45	47.42	26.42	38.00	45.71	57.50
glm-4v-9B (GLM et al., 2024)	53.20	70.41	64.14	69.00	54.65	69.42	44.29	<u>32.91</u>	30.80	43.27	57.50
MiniCPM-V 4.0 (Yao et al., 2024)	53.71	71.72	68.42	<u>67.00</u>	51.74	74.38	42.58	32.29	33.00	49.39	51.00
InternVL2.5-8B (Chen et al., 2024)	52.76	68.52	70.07	60.00	51.74	66.12	45.23	31.24	33.00	44.08	<u>58.00</u>
Qwen2.5-VL-3B (Bai et al., 2025b)	52.88	70.66	65.13	64.00	45.93	71.07	46.13	28.60	33.00	45.71	53.50
Qwen2.5-VL-32B (Bai et al., 2025b)	56.70	74.69	67.76	60.00	57.56	72.73	45.97	35.01	38.20	59.59	54.50
Qwen2.5-VL-72B (Bai et al., 2025b)	56.91	<u>77.38</u>	68.75	52.00	<u>58.14</u>	75.21	<u>46.75</u>	32.08	<u>38.40</u>	<u>60.00</u>	50.00
InternVL3-38B (Zhu et al., 2025)	<u>57.91</u>	75.57	<u>76.32</u>	69.00	54.07	<u>76.86</u>	46.56	32.29	40.40	55.92	56.50
InternVL3-78B (Zhu et al., 2025)	59.43	79.18	77.30	66.50	59.30	80.99	46.01	31.67	40.40	60.82	58.50
Intern-s1 (Bai et al., 2025a)	42.37	63.93	51.97	42.50	40.94	33.06	20.15	32.08	31.00	45.31	43.00
<i>Baseline</i>											
Blind GPT-4o	36.39	58.93	42.43	17.00	17.44	29.75	21.96	29.14	31.60	29.80	25.50
Random Choice	26.93	25.00	25.00	50.00	25.00	25.00	25.00	25.00	25.00	25.00	41.00

Table 3: Benchmark results for MLLMs under the open-ended evaluation setting. For each task, the **best-performance** is indicated in bold and the second-best are underlined.

	Overall	General					Spatial				
		OA	HA	Exist.	Count.	OCR	EVO	AVO	SS	RD	OR
<i>Proprietary MLLMs</i>											
GPT-4o (Hurst et al., 2024)	<u>42.91</u>	<u>52.62</u>	<u>39.74</u>	<u>68.50</u>	45.35	43.80	32.27	27.25	30.30	<u>61.84</u>	<u>49.50</u>
Qwen-VL-Plus (Bai et al., 2025b)	39.87	44.39	39.35	67.50	<u>47.00</u>	36.36	<u>34.39</u>	<u>29.10</u>	27.65	51.09	46.20
Gemini-2.0-flash (Comanici et al., 2025)	36.42	37.82	28.55	48.26	50.00	56.50	30.86	25.89	<u>31.00</u>	55.51	42.17
o3 (OpenAI, 2025)	49.53	55.49	45.36	69.50	50.00	<u>52.89</u>	45.40	34.59	39.60	62.04	59.10
<i>Open-sourced MLLMs</i>											
LLaVA-v1.5-7B (Liu et al., 2024a)	32.29	35.02	32.07	56.50	24.42	9.504	28.28	25.47	26.60	45.10	43.50
LLaVA-ov-0.5B (Li et al., 2024a)	17.90	28.75	11.12	42.00	19.19	3.719	6.196	5.765	8.300	29.18	32.20
idefics3-8B (Laurençon et al., 2024)	27.93	31.50	28.16	65.00	43.60	27.27	16.75	15.41	20.60	37.35	37.90
XComposer2 (Dong et al., 2024)	28.36	30.12	20.92	48.00	34.88	1.652	23.13	25.79	23.00	42.65	43.15
Deepseek-VL-1.3B (Lu et al., 2024)	27.80	31.33	18.22	53.50	33.14	6.198	20.98	19.92	23.10	42.24	44.15
LLaVA-Next-7B (Li et al., 2024b)	30.52	36.58	32.24	60.50	40.12	12.81	21.04	22.01	17.60	38.78	44.45
LLaVA-Next-34B (Li et al., 2024b)	35.25	41.57	29.28	49.50	41.52	7.025	35.40	20.21	24.60	45.51	52.42
glm-4v-9B (GLM et al., 2024)	35.79	38.80	26.12	60.50	42.44	32.23	36.38	25.26	26.50	41.43	42.95
MiniCPM-V 4.0 (Yao et al., 2024)	32.52	36.02	30.56	57.00	43.60	38.43	29.34	24.32	21.04	46.53	36.25
InternVL2.5-8B (Chen et al., 2024)	30.86	33.52	22.34	62.00	39.53	34.71	21.96	25.68	20.40	38.98	51.55
Qwen2.5-VL-3B (Bai et al., 2025b)	38.91	40.80	39.64	<u>63.50</u>	41.86	<u>41.32</u>	<u>35.77</u>	28.09	26.80	47.35	<u>56.20</u>
Qwen2.5-VL-32B (Bai et al., 2025b)	37.67	39.56	26.34	62.00	42.44	30.91	36.47	<u>30.21</u>	<u>30.43</u>	50.41	44.25
Qwen2.5-VL-72B (Bai et al., 2025b)	39.49	45.89	35.14	63.00	42.44	39.55	34.91	24.10	27.60	54.39	47.75
InternVL3-38B (Zhu et al., 2025)	40.96	48.11	39.57	59.00	40.94	38.43	34.66	29.77	27.60	<u>54.08</u>	52.62
InternVL3-78B (Zhu et al., 2025)	42.52	<u>47.05</u>	43.91	62.00	<u>57.56</u>	48.76	35.58	29.77	29.82	53.27	53.95
Intern-s1 (Bai et al., 2025a)	<u>42.12</u>	46.30	<u>41.68</u>	53.50	63.95	40.50	34.72	31.87	30.80	52.04	58.85

4.2 MAIN RESULTS

Close-ended and open-ended performances of all models across all tasks are reported in Table 2 and Table 3, respectively. For the close-ended evaluation, we additionally include GPT-4o without image input (Blind GPT-4o) and chance-level accuracy as baselines for comparison.

4.2.1 OVERALL PERFORMANCE

As illustrated in Table 2, proprietary models achieve the strongest overall performance under both the close-ended and open-ended evaluation settings, where ChatGPT o3 attaining the top overall score of 62.62 and 49.53, respectively. Open-source models also show competitive results, in which Qwen2.5-VL-72B and InternVL3-78B even outperforming GPT-4o. However, the results are still **far from satisfactory**, revealing that current MLLMs still struggle to comprehend the immersive environments presented by omnidirectional images. Besides, the best-performing model (o3) exceeds the Blind GPT-4o baseline by less than 30% accuracy under close-ended setting, suggesting that MLLMs still struggle to comprehend the rich visual information conveyed by ODIs.

4.2.2 TASK-WISE PERFORMANCE

From both the close-ended and open-ended evaluations, it is evident that **ODI spatial understanding is substantially more challenging than general understanding**. For general-level tasks such as attribute recognition, existence verification, and OCR, the complexity of immersive environments increases task difficulty; nevertheless, models can still partially interpret ERP images from a 2D perspective and thereby produce correct answers, which aligns with their already strong capabilities in 2D general-level understanding. However, for tasks more closely related to spatial comprehension, *i.e.*, counting, model performance drops significantly (by about 20% compared with attribute recognition tasks).

The challenge becomes even more pronounced for tasks that fully rely on immersive spatial comprehension. Since current MLLMs are primarily trained on 2D data, their spatial reasoning capabilities are inherently limited. These limitations become especially obvious when it comes to omnidirectional comprehension requiring immersive spatial understanding, where model performance drops greatly compared to general-level tasks, only slightly above the random choice baseline. This issue is particularly evident in non-egocentric spatial reasoning tasks, *i.e.*, allocentric view orientation and scene simulation, which are already difficult in conventional 2D images (Li et al., 2025). In the ODI setting, these tasks pose an even greater challenge, with model performance only marginally surpassing (or even falling below) that of the Blind GPT-4o baseline, suggesting that current models still fall short in capturing the spatial information conveyed by omnidirectional images.

4.3 CLOSED VERSUS OPEN EVALUATION

Comparing Table 2 and Table 3, we observe that model performance differs greatly between closed and open-ended QA settings. The findings demonstrate the necessity for conducting both closed and open-ended benchmarks. For tasks with a unique ground truth, *i.e.*, counting and OCR, we can directly compare their performance across the two tables. The performance of these two tasks generally drops, indicating that *the choices may provide a hint for the MLLMs*. Interestingly, *not all answer choices produce a positive effect*. We observe cases where a model provides a correct response in the open-ended setting but selects the wrong option in the close-ended format. This discrepancy suggests that the presence of predefined options may sometimes introduce interference, and further reflects a potential difference between the model’s generative reasoning in open-ended tasks and its discriminative reasoning in multiple-choice tasks.

We further observe that the model performance divergence is more evident in the open-ended setting, especially on spatial-level tasks, where models exhibit significantly larger variations. Unlike multiple-choice questions, where the given options constrain the answer space, open-ended responses can better reveal the differences between MLLMs’ reasoning and that of humans. For example, in the egocentric view orientation task, when no explicit constraints are imposed, models rarely produce ego orientation terms. Instead, they tend to describe orientations in relative terms. However, even when explicitly instructed to output absolute orientations, the models’ performance remains unsatisfactory. This suggests that MLLMs do not naturally reason about immersive ODI scenes in a human-like manner, *i.e.*, by first engaging in perspective-taking and then conducting relative spatial analysis. Instead, their reasoning still resembles processing a warped 2D image.

5 OMNI-COT: IMPROVING MLLMs UNDERSTANDING OF ODIs

In this section, we propose **Omni-CoT**, a training-free framework for improving MLLMs understanding capabilities on omnidirectional images by leveraging a human-like step-by-step chain-of-thought reasoning strategy, including viewpoint-guided answering, crop cue grounding and refining, and response refinement.

5.1 FRAMEWORK OVERVIEW

5.1.1 VIEWPOINT GUIDED ANSWERING

Unlike conventional images, ODI comprehension requires MLLMs to extract viewpoint cognition from the projected ERP-format images. However, as analysed in Section 4.3, MLLMs often perceive ODIs merely as warped 2D images rather than reasoning within the immersive full-view setting, which poses a significant challenge even for proprietary models. In 2D image comprehension, spatial understanding is often enhanced either through large-scale training or by incorporating prior information generated from 3D models (Yang et al., 2025a; Li et al., 2025). However, training-based approaches are resource-intensive and may overfit to the training data, While 3D-derived features

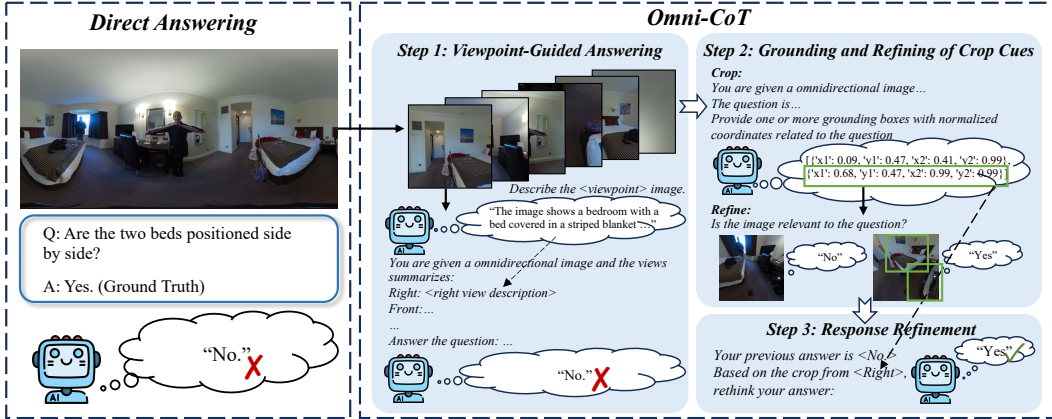


Figure 4: We introduce **Omni-CoT**, The framework enhances VLMs’ comprehension of omnidirectional images via chain-of-thought reasoning through three steps: viewpoint-guided answering, grounding and refinement of crop cues, and response refinement. Compared with direct answering, Omni-CoT achieves notable performance improvements.

can provide useful cues, reliance on external models is often insufficient and not widely applicable. To this end, We aim to explore training-free approaches to enhance MLLMs’ understanding of ODIs by leveraging internal scene information through step-by-step reasoning.

A straightforward approach is to feed ODIs along with the multi-view images splitted from them into MLLMs, effectively guiding the models to view the ODIs in a human-like way by incorporating viewpoint information. However, this approach is not practically feasible, as omnidirectional images inherently have high resolution, combining them with high-resolution multi-view inputs can easily exceed the model’s maximum input capacity, leading to failure. Moreover, high-resolution multi-view inputs generate a large number of image tokens, most of which are redundant or irrelevant, potentially hindering the model’s ability to focus on the critical information within the omnidirectional images.

To this end, we propose a more efficient approach by guiding MLLMs to explore the immersive environment presented by ODIs using compact textual prompts rather than additional image inputs, as presented in Figure 4. Specifically, multi-view images are first extracted from the inverse sphere projection to generate six perspective views, *i.e.*, top, bottom, right, left, front and back. Subsequently, we use the MLLM to generate captions for each of the six viewpoints, capturing the key information contained in each view. By integrating these captions with the corresponding orientation information, the model can acquire a coarse understanding of the surrounding environment, thereby enhancing its global perception of the omnidirectional scene.

5.1.2 CROP CUE GROUNDING AND REFINEMENT

Directly extracting visual information from the full warped ERP image can be challenging for MLLMs. To address this, we propose a crop cue projection strategy. The MLLM is tasked with identifying the most relevant image crops, from which narrow-FoV crops are extracted as low-distortion visual cues to aid ODI comprehension. For a grounding box (x_1, y_1, x_2, y_2) where (x_1, y_1) and (x_2, y_2) represent the normalized coordinates of the top-left and bottom-right corners, respectively, the spherical parameters of the narrow-FoV crop, *i.e.*, the spherical coordinates of the narrow-FoV cue’s center (θ, ϕ) and the approximate FoV fov are computed as:

$$\theta = -180^\circ + \frac{c_x}{W} \cdot 360^\circ, \phi = 90^\circ - \frac{c_y}{H} \cdot 180^\circ, \tag{1}$$

$$fov_w = (x_2 - x_1) \cdot 360^\circ, fov_h = (y_2 - y_1) \cdot 180^\circ, \tag{2}$$

$$fov = \text{clip}\left(\max(fov_w, fov_h) + \text{margin}, 30^\circ, 120^\circ\right) \tag{3}$$

where (c_x, c_y) is the center of the crop, W and H are the width and height of the ERP image, respectively, $margin$ is an optional angular expansion to avoid overly tight cropping, and $\text{clip}(\cdot)$ limits the FoV to a reasonable range.

However, since grounding may not always be accurate, relying solely on it can introduce unnecessary distractors. Therefore, we introduce a refinement mechanism, where the MLLM is queried

Table 4: Performance of Omni-CoT on ODI-Bench, better performances over baseline are **bolded**.

Method	Overall	General					Spatial				
		OA	HA	Exist.	Count.	OCR	EVO	AVO	SS	RD	OR
o3	62.62	75.82	74.01	75.00	57.56	77.69	56.20	39.62	46.60	70.20	59.50
(w/ Viewpoint Guiding)	68.78	75.57	75.66	78.00	55.81	77.69	81.23	41.93	54.80	68.57	62.00
$\Delta(\uparrow)$	+6.16	-0.25	+1.65	+3.00	-1.75	+0.00	+25.03	+2.31	+8.20	-1.63	+2.50
(w/ Omni-CoT)	70.03	76.15	75.66	81.00	64.53	78.51	82.60	42.98	55.20	71.02	62.00
$\Delta(\uparrow)$	+7.41	+0.33	+1.65	+6.00	+6.97	+0.82	+26.40	+3.36	+8.60	+0.82	+2.5
GPT-4o	55.79	74.43	67.76	65.50	49.42	74.38	43.24	32.49	39.60	57.55	53.50
(w/ Viewpoint Guiding)	61.67	73.69	65.28	74.00	54.07	76.03	70.06	37.31	39.80	53.88	56.50
$\Delta(\uparrow)$	+5.88	-0.74	-2.48	+8.50	+4.65	+1.65	+26.82	+4.82	+0.20	-3.67	+3.00
(w/ Omni-CoT)	62.08	73.77	68.42	75.00	54.07	76.03	71.53	37.94	37.60	52.65	58.50
$\Delta(\uparrow)$	+6.17	-0.66	+0.66	+9.50	+4.65	+1.65	+28.29	+5.45	-2.00	-4.90	+5.00
Gemini-2.0-flash	57.12	73.03	69.41	66.50	52.33	80.16	48.10	32.91	40.20	61.13	54.00
(w/ Viewpoint Guiding)	62.95	73.60	68.75	75.50	55.23	83.47	72.64	35.85	41.00	62.45	54.00
$\Delta(\uparrow)$	+5.83	+0.57	-0.66	+9.00	+2.90	+3.31	+24.54	+2.94	+0.8	+1.32	+0.00
(w/ Omni-CoT)	63.89	73.77	69.41	76.50	57.56	84.30	74.36	36.06	42.20	62.45	55.50
$\Delta(\uparrow)$	+6.77	+0.74	+0.00	+10.00	+5.23	+4.14	+26.26	+3.15	+2.00	+1.32	+1.50
Qwen2.5-VL-72B	56.91	77.38	68.75	52.00	58.14	75.21	46.75	32.08	38.40	60.00	50.00
(w/ Viewpoint Guiding)	64.51	76.39	73.02	66.50	55.49	77.87	76.07	37.31	46.61	54.89	51.00
$\Delta(\uparrow)$	+7.60	-0.99	+4.27	+14.50	-2.65	+2.66	+29.32	+5.23	+8.21	-5.11	+1.00
(w/ Omni-CoT)	65.41	76.80	74.01	66.50	54.32	77.87	80.12	37.74	45.20	56.33	51.50
$\Delta(\uparrow)$	+8.50	-0.58	+5.26	+14.50	-3.82	+2.66	+33.37	+5.66	+6.80	-3.67	+1.50
InternVL2.5-8B	52.76	68.52	70.07	60.00	51.74	66.12	45.23	31.24	33.00	44.08	58.00
(w/ Viewpoint Guiding)	55.76	68.77	72.69	63.00	49.42	80.17	52.39	34.38	34.40	48.98	60.50
$\Delta(\uparrow)$	+3.00	+0.25	+2.62	+3.00	-2.32	+14.05	+7.16	+3.14	+1.40	+4.90	+2.5
(w/ Omni-CoT)	58.04	71.48	72.69	63.50	52.33	80.99	58.28	35.64	34.40	49.39	61.50
$\Delta(\uparrow)$	+5.28	+2.96	+2.62	+3.50	+0.59	+13.97	+13.05	+4.40	+1.40	+5.31	+3.50

Table 5: Ablation studies of Omni-CoT on ODI-Bench

Model	Strategy			Performance		
	Viewpoint Guiding	Crop Grounding	Crop Refinement	Overall	General	Spatial
Gemini-2.0-flash				57.12	70.49	45.05
	✓			63.07	72.08	54.94
	✓	✓		62.79	71.79	54.67
	✓		✓	58.29	67.67	49.83
	✓	✓	✓	63.89	72.63	56.01
InternVL2.5-8B				52.76	66.33	40.53
	✓			55.76	67.82	44.88
	✓	✓		53.71	65.79	42.83
	✓		✓	48.93	54.29	44.12
	✓	✓	✓	58.04	69.81	47.43

again to label the relevance of each crop with respect to the question as “yes” or “no”, and only the crops deemed relevant are fed back to the model to assist the response refinement step.

5.1.3 RESPONSE REFINEMENT

Finally, the ODI, along with the viewpoint captions, as well as the crop cues with their orientation information derived from the spherical coordinates, is fed back to assist in refining the response. The model is provided with its previous answer and prompted to rethink the answer based on the crop cues. As illustrated in Figure 4.

5.2 OMNI-COT PERFORMANCE

5.2.1 PERFORMANCE IMPROVEMENT ON ODI-BENCH

We conduct close-ended experiments on o3, GPT-4o, Gemini-2.0-flash, Qwen2.5-VL-72B and InternVL2.5-8B to validate the effectiveness of our framework on both proprietary and open-sourced MLLMs, the results are presented in Table 4. As indicated in the table, viewpoint guiding serves as a key component for performance improvement, especially on spatial-related tasks. Moreover, the models performance could be overall further improved with the aid of crop cues.

5.2.2 ABLATION STUDIES

We conduct ablation experiments to validate the effectiveness of each step in Omni-CoT, with results presented in Table 5. The results indicate that relying on direct grounding and cropping introduces

Table 6: More hyperparameter ablation of **Omni-CoT** on ODI-Bench, best performances are **bolded**.

Method	Overall	General					Spatial				
		OA	HA	Exist.	Count.	OCR	EVO	AVO	SS	RD	OR
GPT-4o	55.79	74.43	67.76	65.50	49.42	74.38	43.24	32.49	39.60	57.55	53.50
Omni-CoT (80° FoV)	60.27	66.39	68.09	74.50	52.91	75.21	73.37	37.73	38.60	52.65	58.00
Omni-CoT (100° FoV)	60.71	67.29	67.11	74.50	54.07	73.55	72.27	37.73	40.40	55.10	60.50
Omni-CoT (90° FoV) (Ours)	62.08	73.77	68.42	75.00	54.07	76.03	71.53	37.94	37.60	52.65	58.50

Table 7: Performance comparison of multi-view input, video input and proposed Omni-CoT, best performances are **bolded**.

Method	Overall	General					Spatial				
		OA	HA	Exist.	Count.	OCR	EVO	AVO	SS	RD	OR
GPT-4o	55.79	74.43	67.76	65.50	49.42	74.38	43.24	32.49	39.60	57.55	53.50
(multi-view input)	56.01	74.10	67.11	71.00	53.49	76.03	45.15	32.91	37.60	52.24	54.00
(w/ Omni-CoT)	62.08	73.77	68.42	75.00	54.07	76.03	71.53	37.94	37.60	52.65	58.50
Gemini-2.0-flash	57.12	73.03	69.41	66.50	52.33	80.16	48.10	32.91	40.20	61.13	54.00
(multi-view input)	54.63	72.95	64.46	46.50	55.81	63.64	49.57	28.30	37.00	55.92	55.50
(video input)	55.34	70.66	67.11	67.00	48.84	67.77	48.59	30.40	36.00	66.12	52.50
(w/ Omni-CoT)	63.89	73.77	69.41	76.50	57.56	84.30	74.36	36.06	42.20	62.45	55.50
InternVL2.5-8B	52.76	68.52	70.07	60.00	51.74	66.12	45.23	31.24	33.00	44.08	58.00
(multi-view input)	51.97	70.49	71.38	62.50	47.67	76.86	39.14	22.22	33.60	51.02	58.00
(video input)	50.63	68.85	71.38	64.00	43.60	61.16	36.32	23.27	34.00	53.88	60.00
(w/ Omni-CoT)	58.04	71.48	72.69	63.50	52.33	80.99	58.28	35.64	34.40	49.39	61.50

unnecessary crops, which can degrade model performance. However, the proposed crop refinement step filters out irrelevant crops, thereby mitigating this negative effect and further boosting performance beyond the baseline with viewpoint guiding. Besides, viewpoint guiding serves as the fundamental component to improve model comprehension of spatial understanding, while crop grounding supplies the model with important visual cues for comprehensive understanding.

We further conduct hyperparameter ablations on GPT-4o to evaluate the effectiveness of the perspective FoV settings in Omni-CoT. As shown in Table 6, using a field of view of 90° leads to the best overall performance, supporting the rationality of our chosen configuration.

5.2.3 COMPARISON EXPERIMENTS

We provide additional baseline comparisons using both multi-view images and video-based inputs. For the multi-view setting, each omnidirectional image is projected into 12 perspective views (front, front-right, right, right-back, back, left-back, left, left-front, top-front, top-back, bottom-front, and bottom-back) and fed into the VLMs along with their orientation information. For the video setting, we convert each omnidirectional image into a 12-second, 60-FPS video that smoothly rotates through the front, right, back, left, and front views, followed by the top and bottom views. Besides, in Table 7 in the supplementary material, we compare the performance of Zero-shot CoT with our proposed Omni-CoT.

The results are presented in Table 7. Though multi-view and video-based inputs offer improvements on relative-direction and ODI reasoning tasks, they do not yield clear overall performance gains. Besides, their effectiveness is further limited by the models’ inherent constraints in handling multi-image or video inputs. While Zero-shot CoT provides minimal improvements on model performance, no clear improvement is observed in spatial-level tasks. In contrast, Omni-CoT consistently achieves the best results across all evaluated models, demonstrating its effectiveness and superiority over other inference pipelines. The experiment further highlights the necessity of our dedicated reasoning strategies tailored for omnidirectional image understanding.

6 CONCLUSION

In this work, we introduce ODI-Bench, a comprehensive benchmark for evaluating MLLMs’ ability to understand immersive environments presented by omnidirectional images. ODI-Bench consists of 2,000 high-quality omnidirectional images and over 4,000 question-answering pairs spanning 10 fine-grained tasks, covering both general-level and spatial-level understanding. We benchmark 20 leading MLLMs using both close-ended and open-ended evaluation settings. Our in-depth analysis of the experimental results reveals that current MLLMs still underperform on omnidirectional image understanding. To address this, we further propose Omni-CoT, a training-free approach to enhance MLLMs’ comprehension on omnidirectional images through chain-of-thought reasoning. Overall,

ODI-Bench provides a rigorous yardstick for both evaluating and improving MLLMs on immersive environment understanding presented by ODIs.

ACKNOWLEDGEMENT

This work was supported in part by the National Natural Science Foundation of China under Grants 62401365, 62225112, 62271312, 62132006, U24A20220, and in part by the China Postdoctoral Science Foundation under Grants BX20250411, 2025M773473.

ETHICS STATEMENT

Our work adheres to the ICLR Code of Ethics. This work introduces ODI-Bench, a benchmark for evaluating MLLMs understanding on omnidirectional images, and Omni-CoT, a training-free framework to enhance comprehension in immersive environments. All images in ODI-Bench are sourced from publicly available web resources under permissible use, with no personally identifiable information or sensitive data are included. Annotation was conducted by domain experts using VR devices, and only consensually verified QA pairs were retained to ensure annotation reliability. Our benchmark is intended purely for academic research and evaluation, and does not involve animal subjects, medical data, or applications in high-risk domains. We carefully considered potential societal impacts, including risks of misuse, and aim to provide the community with a transparent and rigorous tool for assessing VLMs’ capabilities in immersive environments, while promoting responsible stewardship of AI research.

REPRODUCIBILITY STATEMENT

We have made efforts to ensure the reproducibility of our work. The main paper provides a detailed description of the construction process of ODI-Bench (Section 3), including task definitions and evaluation settings (Section 4.1), and clearly outlines the design of the proposed Omni-CoT framework (Section 5.1). In Appendix E, we provide the core prompts used in our experiments to facilitate replication. The dataset construction pipeline, annotation protocol, and evaluation methodology are all described in detail in the main text and supplementary materials. Together, these resources aim to provide sufficient transparency and guidance to reproduce our experimental results. We also plan to release the dataset and code upon publication.

REFERENCES

- Lei Bai, Zhongrui Cai, Maosong Cao, Weihan Cao, Chiyu Chen, Haojiong Chen, Kai Chen, Pengcheng Chen, Ying Chen, Yongkang Chen, et al. Intern-s1: A scientific multimodal foundation model. *arXiv preprint arXiv:2508.15763*, 2025a.
- Shuai Bai, Keqin Chen, Xuejing Liu, Jialin Wang, Wenbin Ge, Sibao Song, Kai Dang, Peng Wang, Shijie Wang, Jun Tang, et al. Qwen2. 5-vl technical report. *arXiv preprint arXiv:2502.13923*, 2025b.
- Zhe Chen, Weiyun Wang, Yue Cao, Yangzhou Liu, Zhangwei Gao, Erfei Cui, Jinguo Zhu, Shenglong Ye, Hao Tian, Zhaoyang Liu, et al. Expanding performance boundaries of open-source multimodal models with model, data, and test-time scaling. *arXiv preprint arXiv:2412.05271*, 2024.
- Shih-Han Chou, Wei-Lun Chao, Wei-Sheng Lai, Min Sun, and Ming-Hsuan Yang. Visual question answering on 360deg images. In *Proceedings of the IEEE/CVF Winter Conference on Applications of Computer Vision (WACV)*, pp. 1607–1616, 2020.
- Gheorghe Comanici, Eric Bieber, Mike Schaekermann, Ice Pasupat, Noveen Sachdeva, Inderjit Dhillon, Marcel Blistein, Ori Ram, Dan Zhang, Evan Rosen, et al. Gemini 2.5: Pushing the frontier with advanced reasoning, multimodality, long context, and next generation agentic capabilities. *arXiv preprint arXiv:2507.06261*, 2025.

- Xiaoyi Dong, Pan Zhang, Yuhang Zang, Yuhang Cao, Bin Wang, Linke Ouyang, Xilin Wei, Songyang Zhang, Haodong Duan, Maosong Cao, et al. Internlm-xcomposer2: Mastering free-form text-image composition and comprehension in vision-language large model. *arXiv preprint arXiv:2401.16420*, 2024.
- Zihao Dongfang, Xu Zheng, Ziqiao Weng, Yuanhuiyi Lyu, Danda Pani Paudel, Luc Van Gool, Kailun Yang, and Xuming Hu. Are multimodal large language models ready for omnidirectional spatial reasoning? *arXiv preprint arXiv:2505.11907*, 2025.
- Huiyu Duan, Qiang Hu, Jiarui Wang, Liu Yang, Zitong Xu, Lu Liu, Xionghuo Min, Chunlei Cai, Tianxiao Ye, Xiaoyun Zhang, et al. Finevq: Fine-grained user generated content video quality assessment. In *Proceedings of the Computer Vision and Pattern Recognition Conference (CVPR)*, pp. 3206–3217, 2025.
- Team GLM, Aohan Zeng, Bin Xu, Bowen Wang, Chenhui Zhang, Da Yin, Diego Rojas, Guanyu Feng, Hanlin Zhao, Hanyu Lai, Hao Yu, Hongning Wang, Jiada Sun, Jiajie Zhang, Jiale Cheng, Jiayi Gui, Jie Tang, Jing Zhang, Juanzi Li, Lei Zhao, Lindong Wu, Lucen Zhong, Mingdao Liu, Minlie Huang, Peng Zhang, Qinkai Zheng, Rui Lu, Shuaiqi Duan, Shudan Zhang, Shulin Cao, Shuxun Yang, Weng Lam Tam, Wenyi Zhao, Xiao Liu, Xiao Xia, Xiaohan Zhang, Xiaotao Gu, Xin Lv, Xinghan Liu, Xinyi Liu, Xinyue Yang, Xixuan Song, Xunkai Zhang, Yifan An, Yifan Xu, Yilin Niu, Yuantao Yang, Yueyan Li, Yushi Bai, Yuxiao Dong, Zehan Qi, Zhaoyu Wang, Zhen Yang, Zhengxiao Du, Zhenyu Hou, and Zihan Wang. Chatglm: A family of large language models from glm-130b to glm-4 all tools, 2024.
- Daya Guo, Dejian Yang, Haowei Zhang, Junxiao Song, Ruoyu Zhang, Runxin Xu, Qihao Zhu, Shirong Ma, Peiyi Wang, Xiao Bi, et al. Deepseek-r1: Incentivizing reasoning capability in llms via reinforcement learning. *arXiv preprint arXiv:2501.12948*, 2025.
- Aaron Hurst, Adam Lerer, Adam P Goucher, Adam Perelman, Aditya Ramesh, Aidan Clark, AJ Ostrow, Akila Welihinda, Alan Hayes, Alec Radford, et al. Gpt-4o system card. *arXiv preprint arXiv:2410.21276*, 2024.
- Takeshi Kojima, Shixiang Shane Gu, Machel Reid, Yutaka Matsuo, and Yusuke Iwasawa. Large language models are zero-shot reasoners. *Advances in Neural Information Processing Systems (NeurIPS)*, 35:22199–22213, 2022.
- Hugo Laurençon, Andrés Marafioti, Victor Sanh, and Léo Tronchon. Building and better understanding vision-language models: insights and future directions., 2024.
- Bo Li, Yuanhan Zhang, Dong Guo, Renrui Zhang, Feng Li, Hao Zhang, Kaichen Zhang, Peiyuan Zhang, Yanwei Li, Ziwei Liu, et al. Llava-onevision: Easy visual task transfer. *arXiv preprint arXiv:2408.03326*, 2024a.
- Dingming Li, Hongxing Li, Zixuan Wang, Yuchen Yan, Hang Zhang, Siqu Chen, Guiyang Hou, Shengpei Jiang, Wenqi Zhang, Yongliang Shen, et al. Viewspatial-bench: Evaluating multi-perspective spatial localization in vision-language models. *arXiv preprint arXiv:2505.21500*, 2025.
- Feng Li, Renrui Zhang, Hao Zhang, Yuanhan Zhang, Bo Li, Wei Li, Zejun Ma, and Chunyuan Li. Llava-next-interleave: Tackling multi-image, video, and 3d in large multimodal models. *arXiv preprint arXiv:2407.07895*, 2024b.
- Chenfei Liao, Wensong Wang, Zichen Wen, Xu Zheng, Yiyu Wang, Haocong He, Yuanhuiyi Lyu, Lutao Jiang, Xin Zou, Yuqian Fu, et al. Are we using the right benchmark: An evaluation framework for visual token compression methods. *arXiv preprint arXiv:2510.07143*, 2025.
- Haotian Liu, Chunyuan Li, Yuheng Li, and Yong Jae Lee. Improved baselines with visual instruction tuning. In *Proceedings of the IEEE/CVF Conference on Computer Vision and Pattern Recognition (CVPR)*, pp. 26296–26306, 2024a.
- Yang Liu, Ming Ma, Xiaomin Yu, Pengxiang Ding, Han Zhao, Mingyang Sun, Siteng Huang, and Donglin Wang. Ssr: Enhancing depth perception in vision-language models via rationale-guided spatial reasoning. *arXiv preprint arXiv:2505.12448*, 2025.

- Yuan Liu, Haodong Duan, Yuanhan Zhang, Bo Li, Songyang Zhang, Wangbo Zhao, Yike Yuan, Jiaqi Wang, Conghui He, Ziwei Liu, et al. Mmbench: Is your multi-modal model an all-around player? In *European Conference on Computer Vision (ECCV)*, pp. 216–233. Springer, 2024b.
- Haoyu Lu, Wen Liu, Bo Zhang, Bingxuan Wang, Kai Dong, Bo Liu, Jingxiang Sun, Tongzheng Ren, Zhuoshu Li, Hao Yang, et al. Deepseek-vl: towards real-world vision-language understanding. *arXiv preprint arXiv:2403.05525*, 2024.
- OpenAI. o3 and o4-mini system card. <https://cdn.openai.com/pdf/2221c875-02dc-4789-800b-e7758f3722c1/o3-and-o4-mini-system-card.pdf>, 2025. Accessed: 2025-08-28.
- Tianhe Ren, Shilong Liu, Ailing Zeng, Jing Lin, Kunchang Li, He Cao, Jiayu Chen, Xinyu Huang, Yukang Chen, Feng Yan, et al. Grounded sam: Assembling open-world models for diverse visual tasks. *arXiv preprint arXiv:2401.14159*, 2024.
- Jason Wei, Xuezhi Wang, Dale Schuurmans, Maarten Bosma, Fei Xia, Ed Chi, Quoc V Le, Denny Zhou, et al. Chain-of-thought prompting elicits reasoning in large language models. *Advances in Neural Information Processing Systems (NeurIPS)*, 35:24824–24837, 2022.
- Jihan Yang, Shusheng Yang, Anjali W Gupta, Rilyn Han, Li Fei-Fei, and Saining Xie. Thinking in space: How multimodal large language models see, remember, and recall spaces. In *Proceedings of the Computer Vision and Pattern Recognition Conference (CVPR)*, pp. 10632–10643, 2025a.
- Liu Yang, Huiyu Duan, Yucheng Zhu, Xiaohong Liu, Lu Liu, Zitong Xu, Guangji Ma, Xionghuo Min, Guangtao Zhai, and Patrick Le Callet. Omni²: Unifying omnidirectional image generation and editing in an omni model. *arXiv preprint arXiv:2504.11379*, 2025b.
- Senqiao Yang, Junyi Li, Xin Lai, Bei Yu, Hengshuang Zhao, and Jiaya Jia. Visionthink: Smart and efficient vision language model via reinforcement learning. *arXiv preprint arXiv:2507.13348*, 2025c.
- Yuan Yao, Tianyu Yu, Ao Zhang, Chongyi Wang, Junbo Cui, Hongji Zhu, Tianchi Cai, Haoyu Li, Weilin Zhao, Zhihui He, et al. Minicpm-v: A gpt-4v level mllm on your phone. *arXiv preprint arXiv:2408.01800*, 2024.
- Weihao Yu, Zhengyuan Yang, Linjie Li, Jianfeng Wang, Kevin Lin, Zicheng Liu, Xinchao Wang, and Lijuan Wang. Mm-vet: Evaluating large multimodal models for integrated capabilities. *arXiv preprint arXiv:2308.02490*, 2023.
- Xu Zheng, Chenfei Liao, Ziqiao Weng, Kaiyu Lei, Zihao Dongfang, Haocong He, Yuanhuiyi Lyu, Lutao Jiang, Lu Qi, Li Chen, et al. Panorama: The rise of omnidirectional vision in the embodied ai era. *arXiv preprint arXiv:2509.12989*, 2025.
- Yikang Zhou, Tao Zhang, Dizhe Zhang, Shunping Ji, Xiangtai Li, and Lu Qi. Dense360: Dense understanding from omnidirectional panoramas. *arXiv preprint arXiv:2506.14471*, 2025.
- Jinguo Zhu, Weiyun Wang, Zhe Chen, Zhaoyang Liu, Shenglong Ye, Lixin Gu, Hao Tian, Yuchen Duan, Weijie Su, Jie Shao, et al. Internvl3: Exploring advanced training and test-time recipes for open-source multimodal models. *arXiv preprint arXiv:2504.10479*, 2025.



Figure 5: Illustration of omnidirectional image browsing. The ODI is viewed using a VR head-mounted display, with the corresponding viewpoints on the ERP projection shown in the right panel.

A OMNIDIRECTIONAL IMAGE VIEWING

Captured by 360° cameras, ODIs provide a full field of view, which is significantly wider than that of a pinhole camera. Consequently, ODIs capture the entire surrounding environment with richer spatial information compared to traditional planar images. Due to their capability of delivering immersive experiences and complete perspectives, ODIs have been widely applied in various domains such as augmented reality (AR), virtual reality (VR), autonomous driving, and robotic navigation. In practice, raw ODI data are typically represented using equirectangular projection (ERP) or cubemap projection (CP) to ensure consistency with imaging pipelines. As a new data modality, ODIs possess both unique advantages (wide field of view enabled by spherical imaging, rich geometric cues, and flexible projection formats) and challenges (severe distortions in ERP and content discontinuity in CP). These characteristics make panoramic vision research both valuable and challenging. In this paper, we mainly focus on ERP-based ODIs, which are the most common format in real-world applications.

ERP provides a direct and simple way of representation. However, due to non-uniform sampling, scene objects are distorted depending on their relative positions in the image, with severe stretching near the poles of the sphere. In real-world applications, ERP-formatted omnidirectional images are typically viewed through VR headmounted devices to create a fully immersive browsing experience, as shown in Figure 5. Based on spherical coordinate projection with the $FoV = 90^\circ$, one can roughly localize the viewer’s front, back, left, right, top, and bottom orientations. This viewing mode is significantly different from that of 2D viewing, thereby introducing challenges for ODI understanding.

B MORE DETAILS OF ODI-BENCH

In this section, we provide more details of our ODI-Bench. We provide one example of each tasks to better illustrate task in Figure 6 and Figure 7.

B.1 DETAILED TASK DESCRIPTION

Object Attribute This task challenges the MLLMs to localize the asked instance from high-resolution warped images and extract the attribute features from it. This task mainly focus on object-level attribute, *e.g.*, color, shape, material, functions, *etc.*

Human Attribute This task challenges MLLMs beyond surface-level attribute recognition by requiring an understanding of human emotions. It encompasses human action recognition, human pose estimation, and even more demanding aspects such as human emotion recognition, *etc.*

Existence This task evaluates a MLLM’s ability to recognize the existence of objects within high-resolution, complex spatial environments with massive instances. Unlike attribute-related questions, it requires the model to reason about the absence of objects. In our experiments, we observe that MLLMs generally perform poorly on existence-related questions.

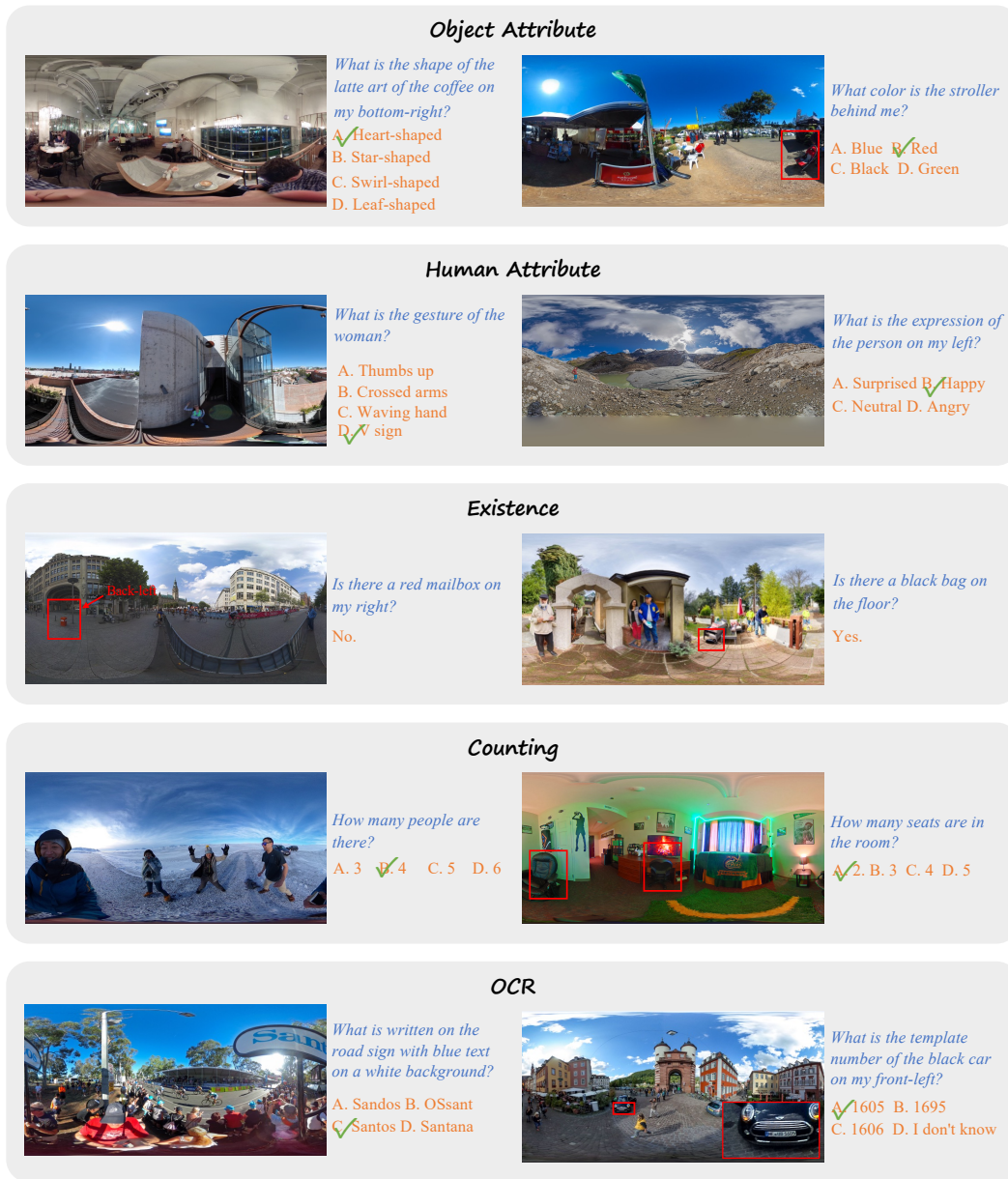


Figure 6: Examples of general-level tasks in ODI-Bench.

Counting Unlike conventional 2D images, ODI counting poses greater challenges as it requires MLLMs to count in a full immersive view, which introduces two major challenges. First, identifying instances from warped viewpoints is inherently difficult, especially with splitted back views introduce distracting information. Second, the omnidirectional environment contains an overwhelming amount of visual information, making the counting task substantially more challenging than in standard 2D images.

OCR Given the inherent characteristics of ODI images, we aim to examine whether the OCR task presents distinct or greater challenges for MLLMs. We design this task as a general evaluation of MLLMs’ capability in ODI understanding. The primary difficulties arise from the need to comprehend high-resolution imagery, accurately ground the referenced text, and to handle viewpoint-induced hallucinations, as illustrated in the example shown in Figure 6.

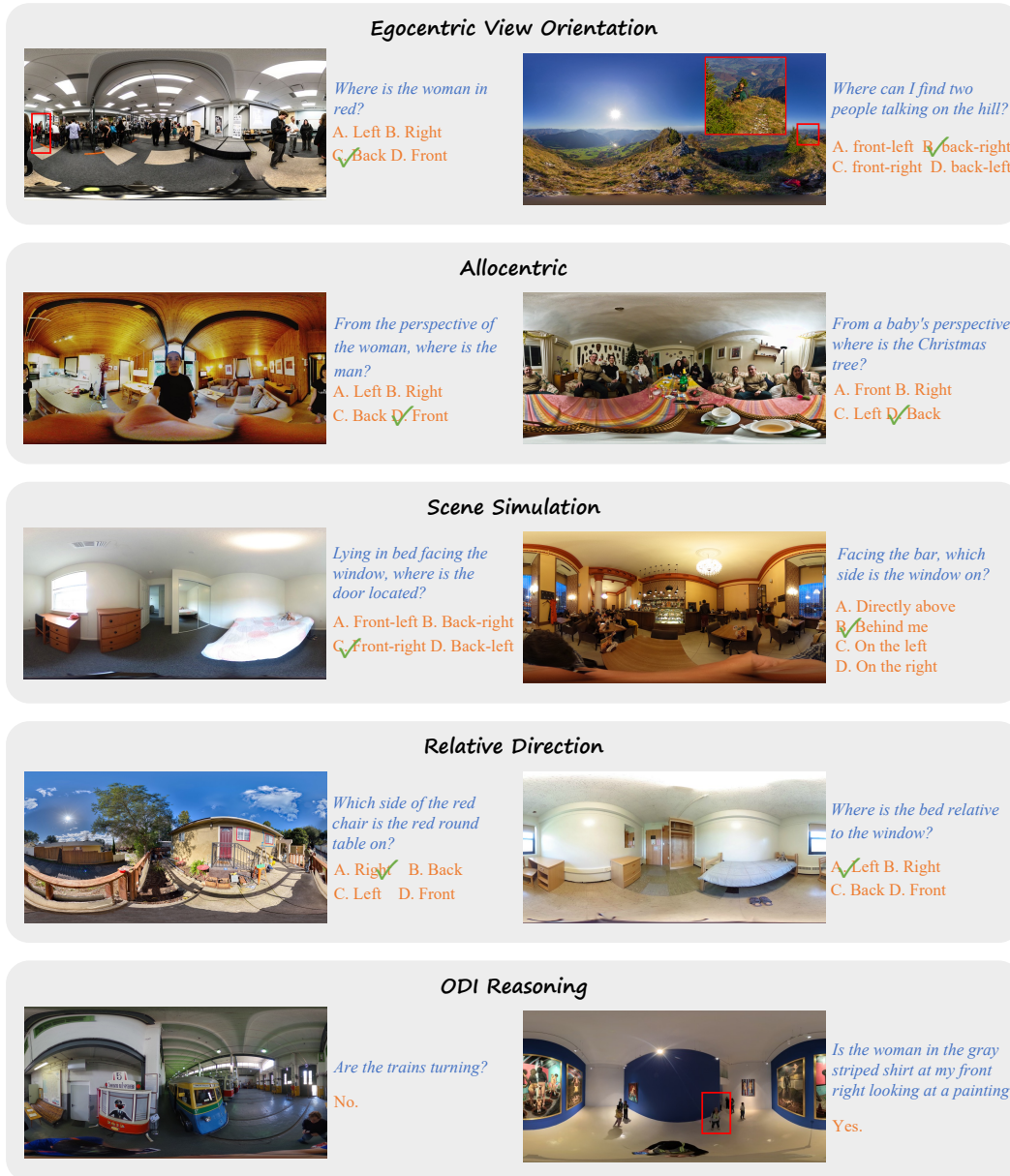


Figure 7: Examples of spatial-level tasks in ODI-Bench.

Egocentric View Orientation Conventional 2D images or N FoV videos only expose viewers to the frontal perspective. In contrast, browsing omnidirectional images inherently requires a 360-degree viewing experience, demanding that MLLMs browse the scene in a human-like manner. The most direct manifestation of this requirement is to specify the orientation of an object (front, back, left, right, up, down) from the viewer’s perspective. This constitutes the most fundamental distinction between omnidirectional image and 2D visual understanding. To this end, we propose the egocentric view-orientation task to assess whether MLLMs are capable of interpreting omnidirectional images within an immersive spatial context.

Allocentric View Orientation Spatial understanding from the allocentric (*i.e.*, the viewpoint of other agents or a third-person depicted in the image) has been proven challenging in 2D images (Li et al., 2025). In this paper, we seek to evaluate whether the task poses greater challenge in ODI-presented immersive environment. Thus, we propose the Allocentric View-orientation task, in which the MLLM is required to determine the spatial orientation of instances relative to another person in

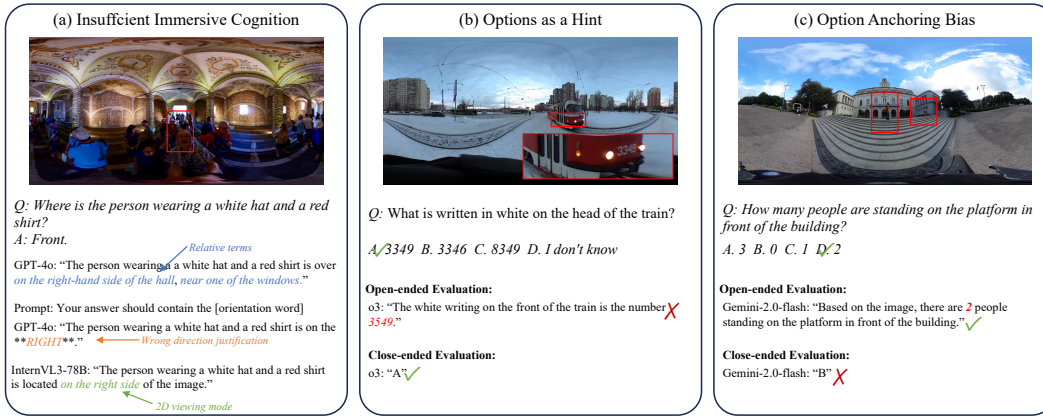


Figure 9: Different error cases in the ODI-Bench.

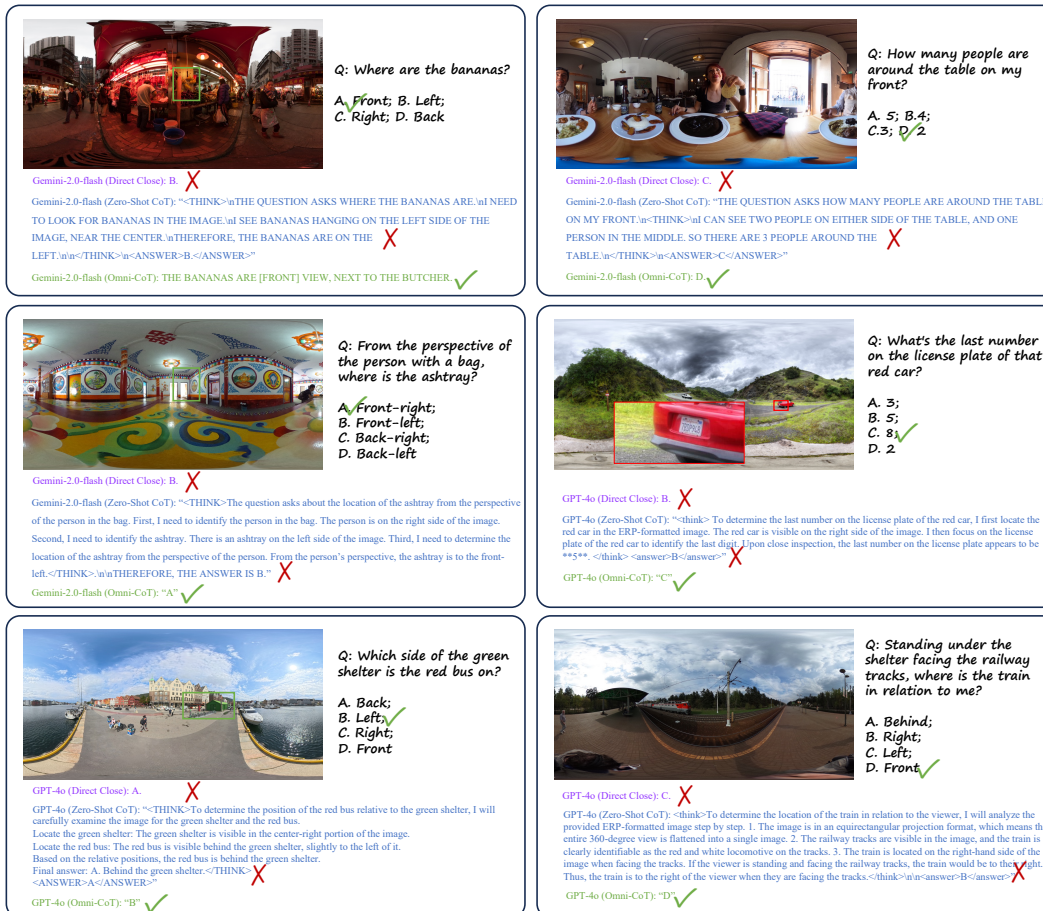


Figure 10: Qualitative examples of direct answering, Zero-shot CoT and proposed Omni-CoT.

D ADDITIONAL EXPERIMENTS

D.1 ERROR CASE ANALYSIS

To gain deeper insights into the bottlenecks of MLLMs for omnidirectional image understanding, we conduct detailed error case analyses based on the close-ended and open-ended evaluation results.

D.1.1 INSUFFICIENT IMMERSIVE COGNITION

As the benchmark results indicate, MLLMs struggle to comprehend the immersive environments captured by omnidirectional images. Specifically, viewpoint information contributes little to their

Table 8: Performance of Zero-shot CoT and Omni-CoT on ODI-Bench, better performances over baseline are **bolded**.

Method	Overall	General					Spatial				
		OA	HA	Exist.	Count.	OCR	EVO	AVO	SS	RD	OR
GPT-4o	55.79	74.43	67.76	65.50	49.42	74.38	43.24	32.49	39.60	57.55	53.50
(w/ Zero-shot CoT)	56.18	73.11	66.12	69.00	54.07	75.21	43.80	37.32	39.40	56.73	52.00
$\Delta(\uparrow)$	+0.39	-1.32	-1.64	+3.50	+4.65	+0.83	+0.56	+4.83	-0.20	-0.82	-1.50
(w/ Omni-CoT)	62.08	73.77	68.42	75.00	54.07	76.03	71.53	37.94	37.60	52.65	58.50
$\Delta(\uparrow)$	+6.17	-0.66	+0.66	+9.50	+4.65	+1.65	+28.29	+5.45	-2.00	-4.90	+5.00
Gemini-2.0-flash	57.12	73.03	69.41	66.50	52.33	80.16	48.10	32.91	40.20	61.13	54.00
(w/ Zero-shot CoT)	57.29	72.70	69.08	70.50	48.26	82.64	49.20	31.87	40.80	61.22	54.50
$\Delta(\uparrow)$	+0.17	-0.33	-0.33	+4.00	-4.07	+2.48	+1.10	-1.04	+0.60	+0.09	+0.50
(w/ Omni-CoT)	63.89	73.77	69.41	76.50	57.56	84.30	74.36	36.06	42.20	62.45	55.50
$\Delta(\uparrow)$	+6.77	+0.74	+0.00	+10.00	+5.23	+4.14	+26.26	+3.15	+2.00	+1.32	+1.50

Table 9: Performance of Omni-CoT on ODI-Bench under the open-ended evaluation setting, better performances over baseline are **bolded**.

Method	Overall	General					Spatial				
		OA	HA	Exist.	Count.	OCR	EVO	AVO	SS	RD	OR
InternVL2.5-8B	30.86	33.52	22.34	62.00	39.53	34.71	21.96	25.68	20.40	38.98	51.55
(w/ Omni-CoT)	36.13	37.71	30.46	67.50	39.53	41.74	33.50	27.46	23.40	42.04	53.50
$\Delta(\uparrow)$	+5.27	+4.19	+8.12	+5.50	+0.00	+7.03	+11.54	+1.78	+3.00	+3.06	+1.95
Gemini-2.0-flash	36.42	37.82	28.55	48.26	50.00	56.50	30.86	25.89	31.00	55.51	42.17
(w/ Omni-CoT)	45.20	38.51	29.41	68.50	52.33	58.26	64.00	33.54	30.70	58.16	44.20
$\Delta(\uparrow)$	+8.78	+0.69	+0.86	+20.24	+2.33	+1.76	+33.14	+7.65	-0.30	+2.65	+2.03

understanding of ODIs, resulting in a noticeable performance decline. As illustrated in Figure 9, the models often respond using relative directions or interpret the ODI as a conventional 2D image, rather than employing orientation terms, even when explicitly instructed to do so. The finding indicates that MLLMs fail to “view” the ODIs like humans do, which poses challenges for ODI understanding. Importantly, this limitation not only hinders spatial-level reasoning but also affects other tasks requiring holistic immersion, such as counting and OCR, as presented in Figure 10.

D.1.2 OPTIONS AS A HINT

Choices serve as a strong prompt for models. Compared with open-ended responses, close-ended evaluation constrains the answer space, which inherently reduces uncertainty. Even when the options are designed to be distracting, they may not target the model’s weak spots, allowing the model to guess the correct answer without truly understanding the content. This short cuts is revealed under open-ended evaluation setting, as presented in Figure 9 (b).

D.1.3 OPTION ANCHORING BIAS

It is common for models to answer correctly in the close-ended setting but fail in the open-ended setting, as the latter presents a much larger solution space. However, we identify an intriguing phenomenon: while the model can provide correct answers in the open-ended setting, it sometimes fails in the close-ended setting by selecting the wrong option, as illustrated in Figure 9 (c), we term this phenomenon as “Option Anchoring Bias”. This observation highlights the necessity of evaluating both close-ended and open-ended settings. Specifically, the close-ended setting examines the model’s ability to ground its reasoning into predefined linguistic expressions, whereas the open-ended setting evaluates the model’s capability to respond in a manner consistent with human immersive viewing of ODIs. These two settings thus complement each other, and a comprehensive assessment should consider both perspectives for a holistic evaluation of MLLMs.

D.2 CAN THINKING LEAD TO BETTER PERFORMANCE?

Following Zero-shot-CoT (Kojima et al., 2022; Wei et al., 2022), we investigate how eliciting step-by-step reasoning from the MLLMs influences model performance on the omnidirectional image understanding tasks. The prompt is presented in Figure 11, we adopt the response format from (Guo et al., 2025) for better thinking and answering extraction. Experiments are conducted with GPT-4o

Table 10: Filter ratio of Crop Refinement Step on GPT-4o.

		<i>General</i>				<i>Spatial</i>				
OA	HA	Exist.	Count.	OCR	EVO	AVO	SS	RD	OR	
35.60%	45.83%	63.96%	49.59%	55.56%	54.44%	45.71%	40.50%	55.90%	45.71%	

Table 11: Performance of simple resizing on ODI-Bench.

<i>Method</i>	<i>Overall</i>	<i>General</i>				<i>Spatial</i>					
		OA	HA	Exist.	Count.	OCR	EVO	AVO	SS	RD	OR
GPT-4o	55.79	74.43	67.76	65.50	49.42	74.38	43.24	32.49	39.60	57.55	53.50
(w/ simple resizing)	54.08	72.70	66.45	60.50	48.83	49.59	43.80	37.32	33.12	56.32	54.00
InternVL3-78B	59.43	79.18	77.30	66.50	59.30	80.99	46.01	31.67	40.40	60.82	58.50
(w/ simple resizing)	55.52	74.43	69.08	60.50	51.16	59.50	42.58	31.67	39.80	60.41	59.00

and Gemini-2.0-flash, and the results for direct answering, Zero-shot CoT, and our Omni-CoT are summarized in Table 8. Qualitative results are presented in Figure 10.

Compared to direct answering, Zero-shot CoT does slightly improve model performance, especially in the existence task. However, the improvement is minimal, and no clear improvement is observed in the spatial-level tasks, which further demonstrate that the model could not effectively utilize the immersive environment information. In comparison, our proposed Omni-CoT effectively boost model performance, especially in the spatial-level tasks, highlighting the effectiveness of our proposed framework.

D.3 FILTERING RATIO OF CROP REFINEMENT STEP

Filtering ratio per task of crop refinement step, a core step in Omni-CoT on GPT-4o is reported in Table 10. Across all tasks, this step successfully removes a substantial amount of redundant information. Together with the results in Table 5, these findings demonstrate that crop refinement significantly contributes to the overall performance improvement.

D.4 OPEN-ENDED EVALUATION RESULTS OF OMNI-COT

We present Omni-CoT on open-ended evaluation setting in Table 9 to further demonstrate the effectiveness of the proposed framework. InternVL2.5-8B and Gemini-2.0-flash are adopted for experiment. Even under unconstrained open-ended setting, Omni-CoT significantly enhances model performance on an overall understanding of omnidirectional images. In particular, Gemini-2.0-flash shows a remarkable improvement of 33.14% on egocentric view orientation task. These results further demonstrate that Omni-CoT greatly improves comprehension on immersive environments presented by ODIs.

D.5 DISCUSSION ON HIGH-RESOLUTION IMAGES

Some recent research (Yang et al., 2025c; Liao et al., 2025) have discussed that in many general scenarios, simple resizing can achieve strong performance. This raises the question of whether such a straightforward technique would also be effective on our ODI-Bench, given that most images in our benchmark are of high resolution. To investigate this, we downsample all images to a resolution of 512×1024 (comparable to that used in previous ODI benchmarks) before feeding them into the MLLMs. We evaluate two strong baseline models, InternVL3-78B and GPT-4o. The corresponding results are presented in Table 11.

For general-level tasks, model performance drops substantially after resizing. This is expected because in the information-dense 360 view, the instances relevant to general tasks typically occupy only a small portion of the entire image. Consequently, resizing blurs these fine-grained regions, leading to significant information loss. This phenomenon is consistent with prior findings in 2D image settings, where OCR-related tasks were shown to be most affected by reductions in input resolution.

Table 12: Performance over multiple runs.

Method	Overall	General					Spatial				
		OA	HA	Exist.	Count.	OCR	EVO	AVO	SS	RD	OR
GPT-4o (round1)	55.79	74.43	67.76	65.50	49.42	74.38	43.24	32.49	39.60	57.55	53.50
GPT-4o (round2)	55.76	75.32	67.11	66.00	49.42	74.38	42.33	33.12	39.00	55.51	54.00
GPT-4o (round3)	55.71	74.43	67.76	65.50	48.84	75.21	42.70	33.96	38.80	56.73	53.50
GPT-4o (mean)	55.75	74.73	67.52	65.67	49.23	74.66	42.76	33.18	39.13	56.59	53.67
GPT-4o (std)	0.04	0.51	0.37	0.29	0.33	0.48	0.46	0.74	0.42	1.02	0.29
InternVL2.5-8B (round1)	52.76	68.52	70.07	60.00	51.74	66.12	45.23	31.24	33.00	44.08	58.00
InternVL2.5-8B (round2)	53.19	69.02	70.39	60.00	51.16	66.94	46.01	31.03	34.20	45.71	56.50
InternVL2.5-8B (round3)	53.24	69.51	71.05	60.50	50.00	67.77	46.01	30.40	33.00	46.94	56.00
InternVL2.5-8B (mean)	53.06	69.02	70.28	60.17	50.96	66.94	45.75	30.89	33.40	45.38	56.83
InternVL2.5-8B (std)	0.26	0.49	0.18	0.28	0.88	0.82	0.45	0.43	0.69	1.44	1.04

Table 13: Comparison of model performance on ODI-Bench under different prompt designs.

	Overall	General					Spatial				
		OA	HA	Exist.	Count.	OCR	EVO	AVO	SS	RD	OR
<i>Prompt: Answer the question based on the provided ERP-formatted image.</i>											
GPT-4o	55.79	74.43	67.76	65.50	49.42	74.38	43.24	32.49	39.60	57.55	53.50
<i>Prompt: This is a 360-degree panoramic image.</i>											
GPT-4o	55.48	74.59	67.43	66.50	48.26	74.38	41.10	32.91	39.60	56.33	55.50
<i>Prompt: This is a 360-degree panoramic image, the image is ERP-formatted.</i>											
GPT-4o	56.06	74.92	65.46	66.00	50.58	73.55	43.80	32.91	40.60	56.73	54.00

In contrast, spatial-level tasks are less affected by token reduction. We hypothesize that these tasks rely more on capturing the global spatial layout rather than fine-grained instance details, allowing the models to maintain relatively stable performance even under reduced image resolution.

D.6 PERFORMANCE OVER MULTIPLE RUNS

We evaluate GPT-4o and InternVL2.5-8B on ODI-Bench by running each model three times and reporting the mean and standard deviation of their performance. The results are presented in Table 12. The performance variation remains within a minimal and acceptable range, further demonstrating the reliability and stability of our benchmark.

D.7 INFLUENCE OF PROMPT

Considering the crucial role of prompts in guiding model understanding, we further explore how different prefix instructions influence model performance. To this end, we experiment with several prompt variants to assess their effects on model performance on ODI-Bench. The results are summarized in Table 13. The performance variation across different prompts remains within a small and acceptable range. Moreover, even when provided with more explicit and descriptive instructions, the models show no substantial improvement on spatial-level tasks. This indicates that relying solely on prompt engineering is insufficient for enabling models to genuinely understand omnidirectional content.

D.8 INFERENCE TIME

Inference time comparison for direct answering, Zero-shot CoT, Omni-CoT (with only viewpoint guiding), and the full Omni-CoT pipeline is reported in Table 14. The experiments are conducted on both InternVL2.5-8B and o3. As shown in the results, Omni-CoT (only w/ viewpoint guiding) incurs only a slightly higher inference time than Zero-shot CoT, yet delivers substantially better overall performance. Furthermore, the full Omni-CoT pipeline brings additional performance gains with a reasonable increase in computation cost.

E PROMPTS

In this section, we present the prompts used throughout the benchmark construction and benchmark experiment.

Table 14: Inference time of direct answering, Zero-shot CoT and Omni-CoT.

		Direct Answering	Zero-shot CoT	Omni-CoT (only w/ viewpoint guiding)	Full Omni-CoT
InternVL2.5-8B	Inference Time	3.44s	7.24s	7.67s	13.81s
	Overall Performance	52.76	52.88	55.76	58.04
o3	Inference Time	12.21s	14.81s	21.11s	35.03s
	Overall Performance	62.62	63.89	68.78	70.03

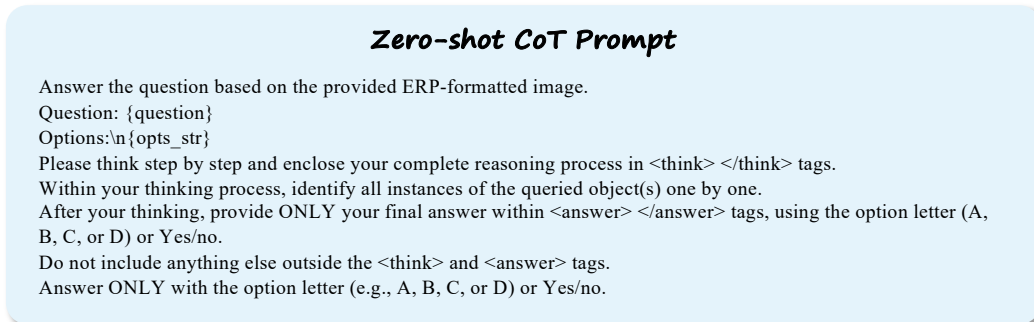


Figure 11: Prompts adopted for Zero-shot CoT.

E.1 BENCHMARK CONSTRUCTION PROMPTS

Prompts are adopted in the automatic data curation pipeline as well as the distractor generation process. The prompts are as presented in Figure 13.

E.2 BENCHMARK PROMPTS

Prompts adopted in the close-ended and open-ended benchmark experiment are shown in Figure 12. For close-ended evaluation, slightly different prompts are employed to ensure the output format of the responses. For open-ended evaluation, due to the fact that models may overlook the immersive environmental perspective and instead tend to answer in a relative direction manner, we explicitly require them to answer with an [orientation word], forcing them to respond starting with a egocentric view orientation expression.

E.3 LLM EVALUATOR PROMPTS

For open-ended responses, we adopted LLM-based evaluator to score the response between 0 to 1. Specifically, we leverage GPT-4o to assist evaluation using a instruction-based prompting approach. As detailed in Figure 14, we cover examples that are fully correct (*i.e.*, 1.0) or incorrect (*i.e.*, 0.0), as well as examples used to define different types of “partially correct” responses. Different evaluation prompts are adopted based on tasks.

For answers with a unique ground truth, *i.e.*, counting and existence, only the key answers strictly aligns with the output is rated as “correct”, else rated as “incorrect”. However, for OCR task, we do not adopt this binary scheme. Instead, answers with correctly recognized characters but in an incorrect order are assigned a partial score of 0.5, in order to further distinguish the model’s OCR capability. While for attribute-level responses, the answers are rated based on the similarity between the key content and the ground truth. In addition, the original question is also taken into account when judging the model’s responses, so as to ensure a more accurate and context-aware evaluation.

For tasks related to direction-based output, *e.g.*, egocentric view orientation and relative direction, *etc.*, we adopt a instruction-based prompting strategy to guide the scoring process. Specifically, if the model’s prediction deviates from the ground-truth orientation by 45 degrees, a partial score of 0.5 is assigned; if it is completely correct, a full score of 1 is given; otherwise, the score is 0.

E.4 OMNI-COT PROMPTS

Prompts for our proposed Omni-CoT are presented in Figure 15.

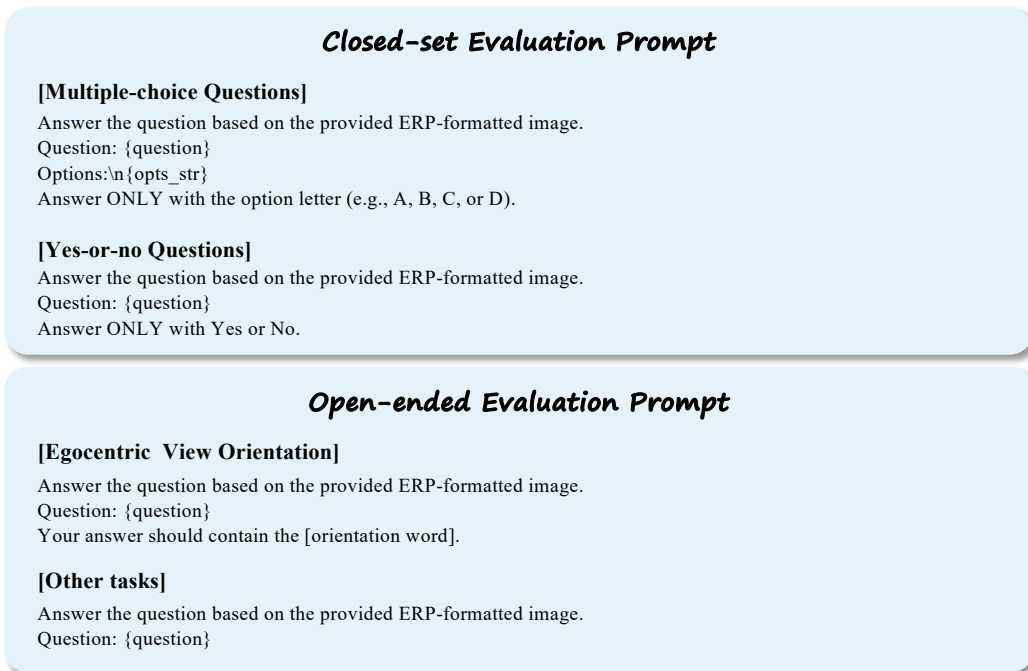


Figure 12: Prompts adopted in closed-set and open-ended evaluation experiments.

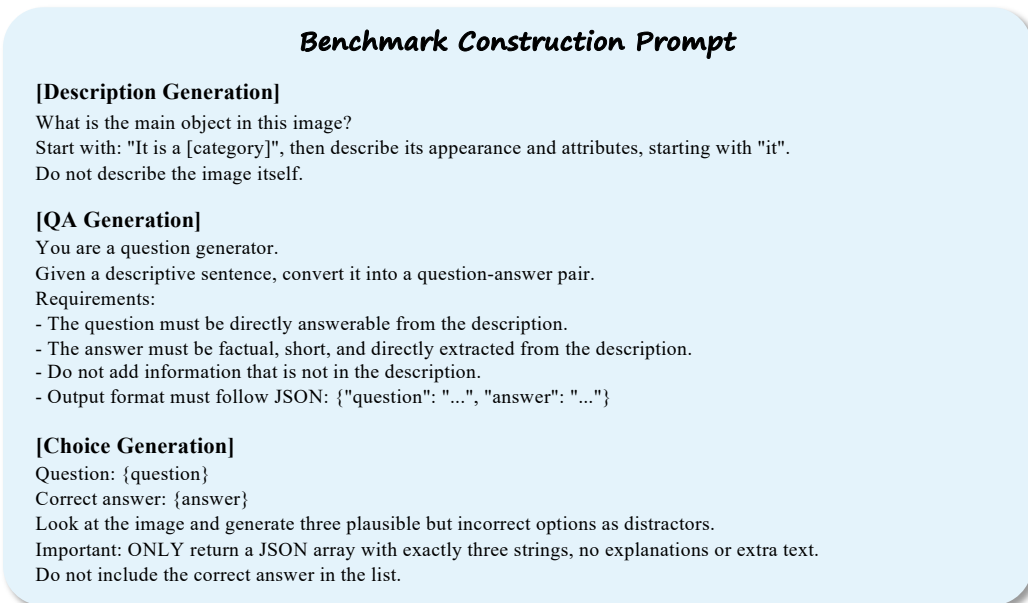


Figure 13: Prompts adopted during the benchmark construction process.

F BROADER IMPACTS

ODI-Bench provides a promising direction for real-world applications by comprehensively evaluating MLLMs on omnidirectional image understanding. By assessing both general-level and spatial-level understanding, we aim to contribute to the advancement of MLLMs towards more immersive and context-aware perception. The general-level tasks, such as attribute recognition, existence, and OCR, are closely aligned with key applications of omnidirectional vision in autonomous driving, VR/AR-based human-computer interaction, and robotic navigation. The spatial-level tasks encourage accurate orientation reasoning, supporting safety-critical applications like navigation and autonomous driving. In particular, the allocentric view orientation and scene simulation tasks contribute to embodied intelligence research, as they equip agents with the ability to reason about unseen

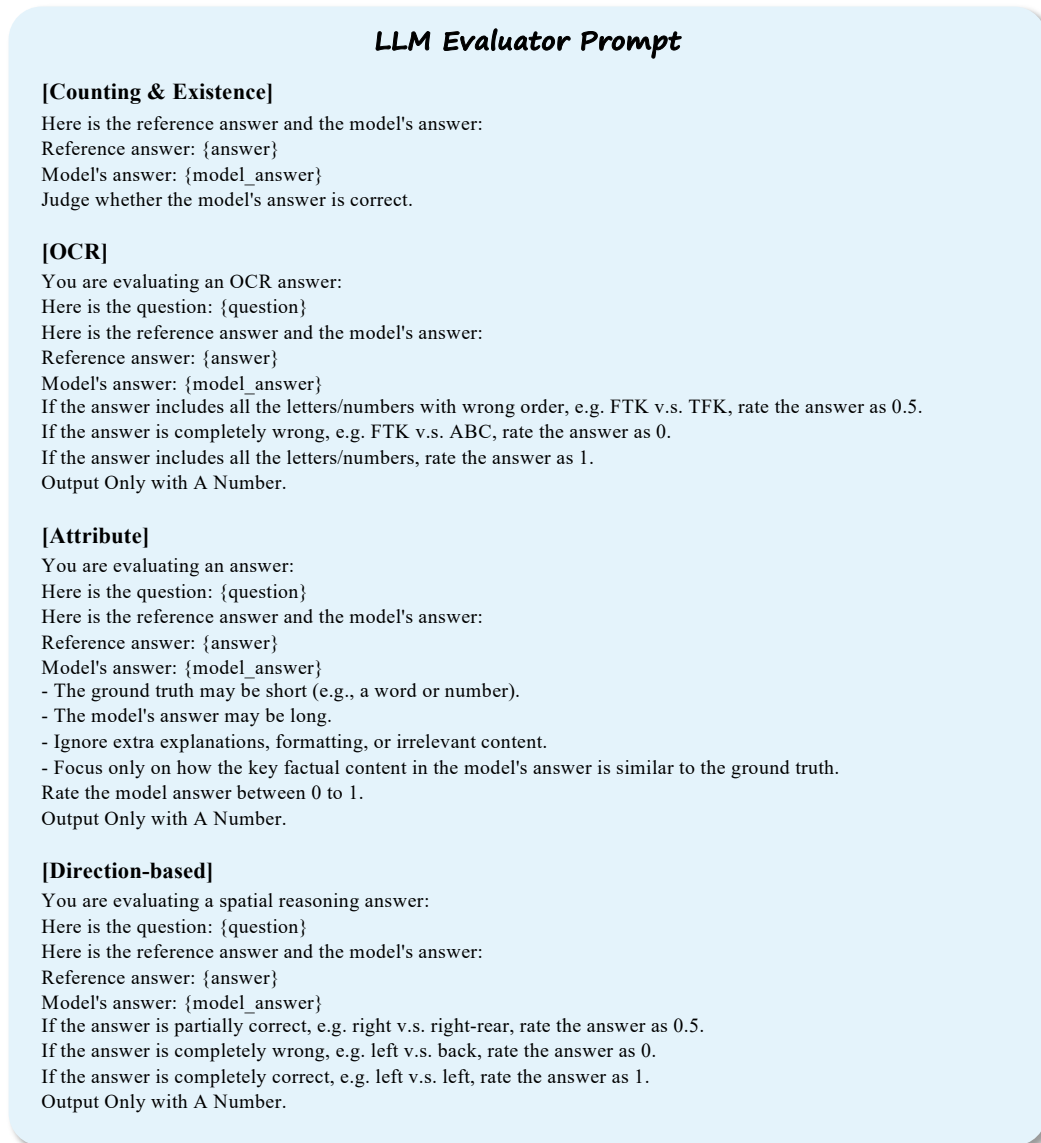


Figure 14: Prompts adopted for the LLM-based evaluator.

viewpoints, reconstruct spatial layouts, and simulate the environment for planning and decision-making.

Beyond serving as an evaluation benchmark, the richness of our data and the diversity of question types also make ODI-Bench a valuable resource for pre-training and post-training of MLLMs. Leveraging ODI-Bench can effectively enhance models' understanding of immersive environments and improve their generalization capabilities in such settings.

G DATA LICENSE

All images in our benchmark are sourced from Flickr under licenses that permit redistribution and academic use. In accordance with these licenses, we only include images that are legally allowed for reuse in research settings. The entire benchmark will be released under the CC BY 4.0 license, enabling free use and redistribution with proper attribution.

Omni-CoT Prompt

[Viewpoint Captioning]

You are given a <view_name> perspective image from an omnidirectional image.
Please provide a detailed caption focusing on key objects or entities visible.
The caption should be No More Than 3 sentences.

[Viewpoint-Guided Answering]

You are given an ERP-formatted omnidirectional image and its perspective view summaries:
{Front View: ...
Right View: ...
...
}
Now answer the following question: <question>
Options: <options>
Answer ONLY with the option letter (e.g. A, B, C, or D).

[Crop Refinement]

Here is a cropped region from an omnidirectional image:
(orientation: <orientation>).
Question: {question}
Is this crop relevant to answering the question?
Answer ONLY with 'Yes' or 'No'.

[Response Refinement]

...
You previously answered: <model_answer> for the question: <question>
Options: <Options>.
Now you are given cropped region(s) focused on the boxes above.
Each crop comes with its approximate orientation (e.g., front, left, top).
Using these crops, either CONFIRM your previous answer or CORRECT it.
If the crops are useless or unclear, output your previous answer exactly as it was.
Output ONLY the final answer (choice letter or yes or no).
Do NOT change your answer unless you are confident!

Figure 15: Prompts adopted in Omni-CoT.

H LLM USAGE STATEMENT

Large Language Models (LLMs) were only used as an assistive tool for minor language polishing and improving readability of the manuscript. All aspects of research ideation, benchmark construction, method design, implementation, data collection, and analysis were conducted entirely by the authors. No part of the research design, experimental process, or analysis was generated by LLMs. The authors take full responsibility for all content of this paper.